Viscoelasticity and crystallization of poly(ethylene oxide) star polymers of varying arm number and size

Salvatore Coppola and Nino GrizzutiGeorge FloudasDimitris Vlassopoulos

Citation: Journal of Rheology **51**, 1007 (2007); doi: 10.1122/1.2751076
View online: http://dx.doi.org/10.1122/1.2751076
View Table of Contents: http://sor.scitation.org/toc/jor/51/5
Published by the The Society of Rheology

Viscoelasticity and crystallization of poly(ethylene oxide) star polymers of varying arm number and size

Salvatore Coppola[a] and Nino Grizzuti

Università degli Studi di Napoli "Federico II," Dipartimento di Ingegneria Chimica, Laboratori "Giovanni Astarita" 80125 Napoli, Italy

George Floudas

University of Ioannina, Department of Physics, 45110 Ioannina, Greece and FORTH, Biomedical Research Institute, Ioannina, Greece

Dimitris Vlassopoulos[b]

University of Crete, Department of Materials Science and Technology 71110 Heraklion, Crete, Greece and FORTH, Institute of Electronic Structure and Laser, Heraklion, Crete, Greece

(Received 11 February 2007; final revision received 31 May 2007)

Synopsis

We investigated the linear melt viscoelasticity and the crystallization kinetics of a series of model poly(ethylene oxide) stars with different functionalities ($f=4-32$ arms) and moderately entangled arms (their molecular masses ranging from 5.5 to 12 kg/mol). The limited data in the homogeneous state indicated that the zero-shear viscosity η_0 was adequately described by the Milner–McLeish model for functionalities $f<32$, where the core effect is insignificant; a similar behavior was observed for the recoverable compliance J_e^0 which depended on both the molecular weight and the number of the arms. Below the melting point, the isothermal crystallization was measured with differential scanning calorimetry and rheology, and analyzed in terms of the Avrami theory, expanding over a wide range of temperatures. The results were supported by additional polarizing optical microscopy data and indicated a slower crystallization kinetics of the stars compared to their linear analogues. They showed a strong dependence of the crystallization rate on the arm molecular weight, whereas the available experimental evidence is suggestive of some functionality dependence as well. © *2007 The Society of Rheology.*
[DOI: 10.1122/1.2751076]

I. INTRODUCTION

Star polymers are known to be the simplest model branch polymer, and to this end they have been studied extensively. In particular, their linear viscoelastic properties have been investigated in detail, both theoretically and experimentally, as a function of arm

[a]Present address: Centro Ricerche Elastomeri, Polimeri Europa S.p.A., Ravenna, Italy.
[b]Author to whom correspondence should be addressed; electronic mail: dvlasso@iesl.forth.gr

number (functionality, f) and molecular weight [Milner and McLeish (1997, 1998); Kapnistos *et al.* (1999); Vlassopoulos *et al.* (2001)]. The most studied polymers are amorphous flexible chains, and in particular polyisoprene [Fetters *et al.* (1993); Pakula *et al.* (1996); Qiao *et al.* (2006)], 1,4-polybutadiene (PB) [Roovers (1985, 1991a, 1991b); Toporowski and Roovers (1986); Pakula *et al.* (1998)] and polystyrene (PS) [Masuda *et al.* (1971); Graessley and Roovers (1979); Roovers (1985); Ohta *et al.* (1986); Clarke *et al.* (2006)], although there are reports on other polymers, such as hydrogenated polybutadiene [Raju *et al.* (1979); Pryke *et al.* (2002)], polyisobutylene [Santangelo *et al.* (1999)] and various blends [Watanabe *et al.* (2006)]. It has been observed that in the limit of low functionality f (up to 16 arms or so) the viscoelastic properties of star polymers depend on the arm molecular weight [Vlassopoulos *et al.* (2001)], but not on f; in such a case, the stars relax via arm relaxation. However, for stars with $f \geqslant 32$ a slow mode was observed in addition to the arm relaxation, and attributed to the center-of-mass motion of the whole star [Kapnistos *et al.* (1999)]. This slow mode in stars affects the terminal relaxation, and for $f=32$ it cannot be clearly decoupled from the arm relaxation [Roovers (1991a)]. At the same time, most of the available data concern stars with a high number of entanglements per arm (typically above seven), i.e., in the regime where tube-model theories work well. It seems therefore appropriate to investigate different star polymers with different chemistry as well as intermediate functionalities and arm molecular weights. Besides their rheological interest as model branched systems and their usefulness for the development and evaluation of theoretical models [McLeish (2002, 2003); Slot and Steeman (2005)], star polymers are also of great industrial importance [Zhao *et al.* (2003)].

On the other hand, star polymers can be also viewed as model branched systems (the simplest possible) for studies of polymer crystallization. Branching has important implications in commercial polymers (typically, long chain branched polyethylenes crystallize). The important open problems in this field relate to the mechanism by which polymer chains crystallize [Heck *et al.* (2000); Iwata (2002)], the rheology of polymers during crystallization [Acierno and Grizzuti (2003); Tanner (2003)], the possible analogies among different crystallizing soft matter systems [Strobl (2000)] and the flow-induced crystallization [Floudas *et al.* (2000); Kornfield *et al.* (2002); Lellinger *et al.* (2003); Coppola *et al.* (2004); van Meerveld *et al.* (2004); Hadinata *et al.* (2005); Kumaraswamy (2005); Kumaraswamy *et al.* (1999)]. Furthermore, star-shaped and dendritic biocompatible polymers are of immense importance in drug delivery [Merrill (1992); Fréchet and Hawker (1996); Stiriba *et al.* (2002)].

Systematic studies on the role of the degree of branching and of the branch molecular weight in the crystallization of branched polymers are still lacking, although even recently a number of studies have been carried out on branched polymers [Cheng and Su (1993); Risch *et al.* (1993); Lambert and Phillips (1994); Righetti and Munari (1997); Floudas *et al.* (1998); Chen *et al.* (1999); Jayakannan and Ramakrishnan (1999); Nuñez *et al.* (2004); Bustos *et al.* (2006)]. This is due, in part, to the complexity of the problem and the lack of well-defined branched polymers. Again, star polymers possess a great advantage for such systematic studies, being the simplest polymers of this kind. Nevertheless, the crystallization of star polymers has been considered only in a very limited number of works [Risch *et al.* (1993); Floudas *et al.* (1998); Chen *et al.* (1999); Nuñez *et al.* (2004)]. Floudas *et al.* (1998) focused their attention on the crystallization of a model tri-arm star block copolymer of polystyrene-polyethylene oxide-poly(ε-caprolactone) (PS-PEO-PCL). This semicrystalline star copolymer was investigated by means of small angle x-ray scattering (SAXS), differential scanning calorimetry (DSC), microscopy and rheology. The system was very interesting, albeit complex, given the enthalpic interac-

tions between the unlike blocks and the propensity of both blocks to crystallize with the latter inducing a macrophase separation between unlike crystals. Furthermore, these star copolymers allowed analyzing the effect of the PCL molecular weight but not of the PEO molecular weight and of the functionality on the crystallization kinetics. Nuñez *et al.* (2004) studied by means of DSC and wide angle x-ray scattering (WAXD) a series of PCL stars with different functionalities (8, 24, 32) and arm molecular masses (1600–9200 g/mol). These authors focused their attention on the thermodynamic parameters of the crystallization (crystal thickness and structure, equilibrium melting point). They observed a depression of crystallinity in the star polymers, which was particularly strong in the hyperbranched case and higher equilibrium melting points than those of the linear analogues. Kinetic and thermodynamic parameters of the crystallization of linear and star-branched nylon-6 have been studied by Risch *et al.* (1993) as a function of branch-point functionality and temperature. These authors did not observe any significant difference in bulk crystallization rates as a function of crystallization temperature or absolute crystalline percentage between linear, three-arm and six-arm samples with identical thermal history. Equilibrium melting points obtained from the Hoffman and Weeks (1962) analysis were also reduced in star-branched nylon-6 compared to the linear polymer of comparable molecular weight. Although the general spherulitic superstructure appeared unaffected by increasing branch-point functionality up to six, irregularities in lamellar structure were implied by SAXS experiments on samples with branch-point functionality as low as three. Chen *et al.* (1999) studied the crystallization, melting, and annealing behaviors of three- and four-arm PEO stars. These stars had all identical arm molecular mass (2220 g/mol), just above the PEO entanglement molecular mass (1600 g/mol) [Fetters *et al.* (1994)]. Diffusion in the melt of these star PEOs, as measured by nuclear magnetic resonance, showed that at constant temperature the self-diffusion slows down with increasing functionality. Furthermore, based on WAXD experiments, the authors concluded that these star PEOs possessed monoclinic crystal structures identical to those of linear PEOs, implying that the coupling agents were rejected from the crystals. The overall crystallization rate of the star PEOs, investigated by means of DSC and simultaneous WAXD and SAXS measurements, decreased with increasing crystallization temperature (T_c) and number of arms. However, due to the low molecular weights of the stars with either three or four arms, no definite conclusions on the effects of number of entanglements per arm and functionality could be drawn. The important role of the entanglements on the crystallization behavior (kinetics and final order) of polymers has been widely discussed in the literature [Hoffman (1982); Hoffman and Miller (1988); Hoffman and Miller (1997); Psarski *et al.* (2000); Iwata (2002); Yamazaki *et al.* (2002); Seguela (2005); Yamazaki *et al.* (2006)]. In particular, Hoffman and co-workers [Hoffman (1982); Hoffman and Miller (1988)] developed a theory of polymer crystallization based on the concept that the crystallization driving force "pulls" the chain (or a part of it) from the amorphous bulk on the solid-liquid interface via a reptation-like mechanism. This approach yielded a M_z^{-1} scaling law for the crystallization growth rate, in satisfactory agreement with experimental data for a series of linear polyethylene fractions (M_w from 2.65×10^4 to 2.04×10^5 g/mol). More recently, an experimental method [Psarski *et al.* (2000); Yamazaki *et al.* (2002, 2006)] was proposed to tune entanglement density in the melt. Extended chain single crystals of polyethylene were obtained by means of high-pressure crystallization and subsequently melted for short annealing time ($<$15–20 min) at high temperature (160 °C). In this way, a polymer melt with entanglement density lower than the equilibrium value was obtained, as the complete reentanglement of the extended chains required longer times. It was shown experimentaly that disentangled chains crystallize faster [Psarski *et al.* (2000); Yamazaki *et al.*

(2002, 2006)]. In fact, an exponential dependence of the nucleation rate on the entanglement density was determined, whereas the temperature dependence of the nucleation process was nearly independent of the entanglement density [Yamazaki *et al.* (2002, 2006)]. Very recently McLeish (2007) argued that the free energy barrier that governs the transition from a molten, but only marginally overlapping single crystal state to the equilibrium state, is enhanced as the molecular weight increases; this could explain recent experiments by Rastogi *et al.* (2003), suggesting the creation of heterogeneous polymer melts from the controlled melting of single crystals.

From the preceeding discussion, it becomes evident that semicrystalline PEO star polymers of intermediate functionalities (4–32) and number of entanglements per arm (3–7) are ideal candidates for addressing the issues mentioned above, concerning the viscoelastic properties in the (homogeneous) melt and the kinetics of crystallization as well as their dependence upon chain molecular weight and architecture.

Recently, Comanita *et al.* (1999) synthesized anionically well-characterized star PEOs of varying functionality and arm molecular mass. In this work, we explore the viscoelastic and crystallization behavior of these PEO stars. In line with recent studies on polymer crystallization [Khanna (1993); Floudas and Tsitsilianis (1997); Floudas *et al.* (1998); Pogodina and Winter (1998)], the present investigation relies on rheological measurements to investigate the crystallization kinetics of the stars. Rheology has the advantage of being very sensitive to any structural change that affects the flow behavior. It allows, for example, measuring crystallization kinetics during its early stages with a very small amount of crystallinity developed. Rheological measurements are also helpful when the crystallization at low undercooling has to be detected as in this condition the crystallization is quite slow, which implies low heat flow. Complementary polarizing optical microscopy (POM) and DSC measurements of the crystallization behavior were also carried out and their results were compared with the rheological information.

II. EXPERIMENT

A. Materials

Five samples of poly(ethylene oxide) (PEO) stars and three of linear PEO chains (for comparison) were employed in the present study. The anionic synthesis involved the preparation of a multifunctional preinitiator from which, on activation, the polymerization of the arms started simultaneously; the fast equilibration between OH^- and O^- anions guaranteed the synthesis of narrow molecular weight distribution arms. The arms the EO units were facing outwards and each arm was terminated by a OH group. Further details about the synthetic methodology and characterization of the star PEOs are provided in the reference by Comanita *et al.* (1999). The stars are presented in Table I and characterized by their functionality, f, the polydispersity index, the arm molecular mass M_{arm}, and the number of entanglements $n_e = M_{arm}/M_e$, where M_e is the molecular mass between entanglements (1600 g/mol [Fetters *et al.* (1994)]). Note that, in Table I the linear polymers are considered as effective two-arm "stars" ($f=2$); therefore the "arm" molecular mass reported for the linear polymers corresponds to one half of the weight-average molecular mass M_w of the whole chain.

B. Methods

All rheological measurements were carried out by means of a Rheometric Scientific controlled strain rheometer (ARES-2KFRTN1, equipped with a dual range force rebalance transducer). A parallel plate (diameter 8 mm, sample thickness 0.4–0.8 mm) geometry was used for the crystallization experiments. Note that for some of the rheological

TABLE I. Molecular characteristics of the PEO samples used.

Sample	f	M_w/M_n	M_{arm} [g/mol]	$n_e=M_{arm}/M_e$
32F6	32	1.08	6188	3.8
32F12	32	1.09	11,906	7.3
16F9	16	1.07	8875	5.5
8F11	8	1.07	10,625	6.5
4F5	4	1.06	5475	3.4
L20	2	1.1	10,000	6.2
L23	2	1.15	12,300	7.6
L62	2	1.37	31,000	19.1
L100	2	1.14	47,000	28.9

measurements in the melt state a cone-plate geometry (25 mm, 0.04 rad) was also used. A convection oven with nitrogen gas was used for temperature control, with a tolerance of less than ±0.1 °C. During the thermal history experiments, the gap was always adjusted to account for the pre-calibrated tool (INVAR) thermal expansion.

The structural evolution of the sample during the crystallization process was monitored rheologically using the following experimental protocol (in Fig. 1 a specific case, 16F9, is graphically reported as an example). After an annealing period of 10 min at 348 K, a cooling down to the crystallization temperature T_c was applied (in the case of Fig. 1 it was 326 K). In order to avoid significant undershoots below the T_c, the cooling phase was composed of the following steps: a cooling ramp (−5 K/min) until 333 K, an isothermal period of 600 s and a successive ramp (−3 K/min) until the selected crystallization temperature T_c. The sample was kept at this temperature for a period t_c-t_0 where t_0 is the time at which the crystallization temperature had been achieved. During the whole experimental time a multiple wave dynamic test was performed. This test is equivalent to simultaneous time sweeps at different frequencies for a given temperature. Indeed, the total linear strain applied on the sample is the sum of several independent

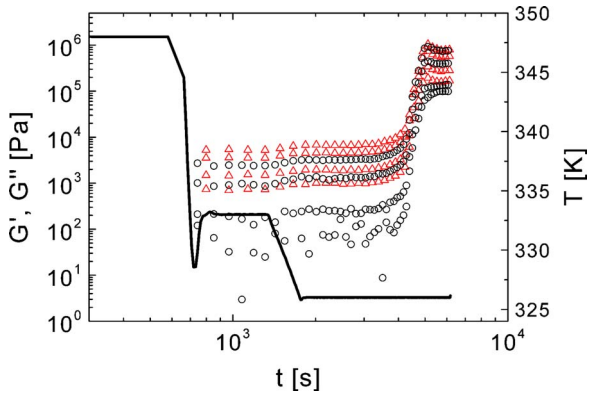

FIG. 1. Evolution of the storage modulus G' (○) and the loss modulus G'' (Δ) during an isothermal crystallization experiment for the sample PEO 16F9. The crossover of the moduli G' and G'' signifies the crystallization transition. From bottom to top, the data correspond to different frequencies (see text): 36, 72, 140, and 270 rad/s. The temperature variation from 348 to 326 K with different cooling rates is also shown with a solid curve in the figure (see text for details).

strain functions, each described by a sinusoidal wave with its own frequency, which is harmonic of the fundamental ω_f (based on the Boltzmann superposition principle). From the stress response to the composite strain, the storage and loss moduli at each discrete frequency are obtained by means of a discrete Fourier transform. Using this technique, the experimental time needed for a single measurement is approximately given by 1.5 periods of the fundamental frequency. It is then possible to sweep a range of approximately three decades of frequencies in a fraction of the time required for a normal dynamic frequency sweep. Therefore, the use of the MultiWave test is particularly advantageous for systems changing with time.

The differential scanning calorimetry (DSC) measurements were performed in a PL-DSC (Rheometric Scientific) with continuous flow of nitrogen gas in order to prevent any thermal degradation of the polymer, and well-defined protocols were followed: the test sample was annealed for 10 min at high temperature (348 K), then quenched to the selected crystallization temperature at rates in the range of 15 K/min and kept there until the isothermal crystallization was completed. By subsequent heating to 348 K at 5 K/min, the temperature corresponding to the endothermic peak (apparent melting temperature, T'_m) was determined.

Polarizing optical microscopy (POM) images were obtained using a Ziess Axioskop 2 optical microscope together with a Linkam heating stage (THMS 600) and a TP93 temperature programmer. The crystallization in real time was followed by a charge coupled device camera (1/2 in. SONY color camera) and a fast frame grabber. The analysis with respect to the nucleation density, growth rates and superstructure shapes were made with an appropriate software (Image Pro Plus). Experiments were made by first heating the samples to 353 K following quenches to different final crystallization temperatures.

III. RESULTS AND DISCUSSION

A. Rheology

The linear viscoelastic characterization of the star and linear PEOs was carried out at 333 K. This temperature is already below the melting point of PEO and is the lowest at which the crystallization is still extremely slow for all the samples. Indeed, in the temperature range 323–329 K crystallization sets in within the period required for the rheological testing. On the other hand, at 333 K the usual range of frequencies available with the rheometer (0.01–100 rad/s) fell already in the terminal flow region of the star PEOs. For this reason there was no need to raise the temperature; besides, the torque was marginal already at 333 K, and it was possible to measure the dynamic moduli over a small frequency range. In particular, we obtained reliable measurements of the storage modulus for only two PEO stars. The dynamic frequency sweep data are depicted in Fig. 2(a) and fall in the terminal region. As already observed in previous works [Graessley and Roovers (1979); Fetters *et al.* (1993)], the dynamic moduli are monotonic functions of the arm molecular weight. At the same time, the behavior of the linear samples also depends strongly on the molecular weight [Doi and Edwards (1986)] (Fig. 2(b)). Again, under the present experimental conditions the terminal region was visible for all samples.

From the available data, the zero-shear viscosity and the recoverable compliance were determined [Ferry (1980)]. The former data are plotted in Fig. 3 (normalized with the plateau modulus and the Rouse time of an entanglement, as discussed below). The results for the linear samples follow expectedly the classical scaling [Doi and Edwards (1986)] with $n_e^{3.4}$ (continuous line in Fig. 3). The values of the viscosities for the stars and the linear chains are in good agreement in the limit of low n_e confirming internal consistency of the data. The data indicate that the main role in determining the zero-shear viscosity is

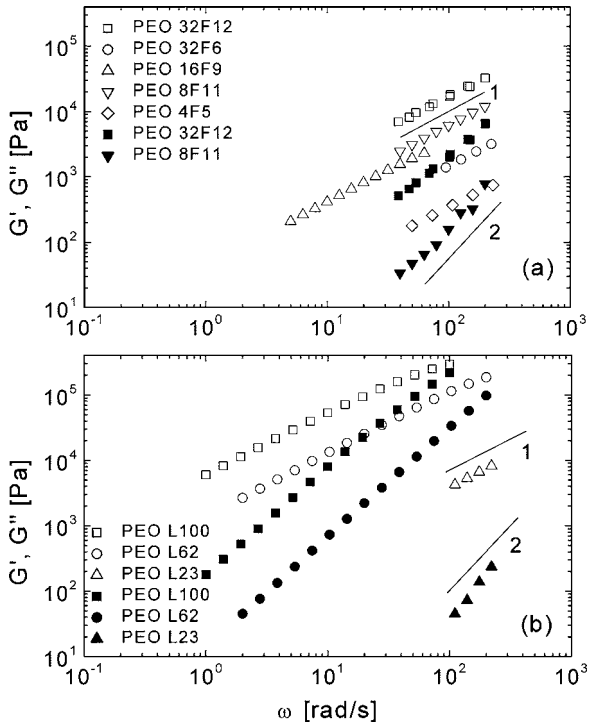

FIG. 2. Dynamic frequency sweeps of star PEO (a) and linear PEO (b) samples at 333 K. Filled symbols: storage modulus, G′. Empty symbols: loss modulus, G″. Lines with slopes 1 and 2 indicate the terminal scaling for G″ and G′, respectively.

played by the arm molecular mass (i.e., the degree of entanglement n_e) but they also suggest that even at these modest degrees of functionality ($f \leqslant 32$) there may be a slight effect of the number of arms on the zero-shear viscosity. A similar behavior was reported for the zero-shear viscosity of 4-, 18- and 32-arm PB stars [Roovers (1985, 1991a); Toporowski and Roovers (1986)]; the zero-shear viscosities of the 32 arm PB stars were indeed higher. For $f \geqslant 64$ the stars' properties were affected by the formation of a soft core [Pakula *et al.* (1998); Kapnistos *et al.* (1999); Vlassopoulos *et al.* (2001)].

A tube-model theory for the stress relaxation in amorphous star polymer melts with low functionality was recently developed by Milner and McLeish (1997, 1998) and proved successful in predicting their viscoelastic behavior [Pakula *et al.* (1998); Kapnistos *et al.* (1999); Santangelo *et al.* (1999); Vega *et al.* (2002)]. This theory has only three parameters, the entanglement molecular weight M_e, the plateau modulus G_N^0 and the Rouse time of an entanglement τ_e. These parameters can be determined from independent measurements on the corresponding linear polymer in the rubbery and transition region, respectively [Milner and McLeish (1997)]. M_e is determined from the plateau modulus through $G_N^0 = 4/5\rho RT/M_e$ [Doi and Edwards (1986)]. In this work, τ_e and M_e could not be determined from the rheological data due to their limited frequency range. Alternatively, τ_e was extracted from the monomeric friction coefficient ζ through the relation $\tau_e = 1/3\pi^2\zeta \cdot N_e^2 b^2/k_B T$ [Doi and Edwards (1986)], where N_e is the number of statistical units per entanglement, b is the statistical segment length, k_B is the Boltzmann's constant and T is the absolute temperature.

In Fig. 3, the normalized zero-shear viscosity data of PEO stars are depicted against

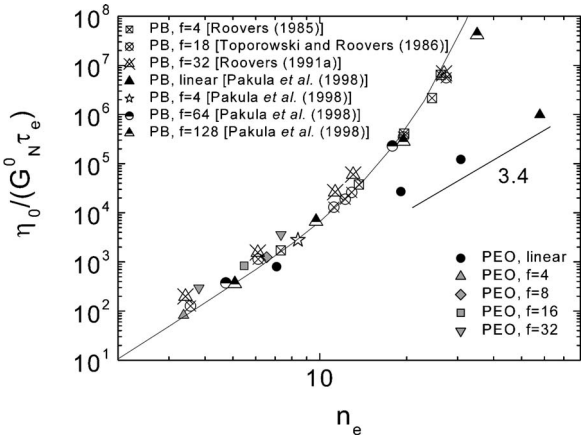

FIG. 3. Zero-shear viscosity (normalized with the plateau modulus and the Rouse time for an entanglement) for linear and star PEOs at 333 K (symbols explained in the bottom right part), plotted against the number of entanglements per arm (a linear polymer is considered as having two arms). Literature data on 1,4-polybutadiene stars [Roovers (1985, 1991a); Toporowski and Roovers (1986); Pakula *et al.* (1998)] are also included for comparison (symbols in top left). Note that the data for the high-functionality PB stars ($f=64$ and 128) correspond to the arm relaxation time, i.e., the earliest of the two terminal modes (the slower being the center-of-mass motion). The line through the data is the Milner-McLeish (1998) theory with a dilution exponent of 4/3.

the number of entanglements per arm, along with respective literature data on PB stars [Roovers (1985, 1991a); Toporowski and Roovers (1986); Pakula *et al.* (1998)]. The Milner-McLeish predictions, indicated with the line through the data and obtained with a dilution exponent of 4/3, are satisfactory. For comparison, the linear PEO data are also included in this figure, and shown to follow the 3.4 scaling. For the PB stars, the experimental values used were self-consistent [Roovers (1985, 1991a); Toporowski and Roovers (1986); Pakula *et al.* (1998)]. For the PEO stars, because of the limited available experimental range, the procedure followed in this work was to retain the value of M_e above and G_N^0 (1.45×10^6 Pa at 333 K) [Fetters *et al.* (1994)] and use the time τ_e as the only adjustable parameter in order to fit the data. Fitting the zero-shear viscosities of the 4 arm star PEO, a value of 3.45×10^{-8} s is extracted; furthermore, using this value, as well as $b=0.73$ nm and $N_e=24.6$, we extract a value for the friction coefficient $\zeta=1.5\cdot10^{-11}$ N s/m. The τ_e and ζ values are very close to those obtained (5.4×10^{-8} s and $2.29\cdot10^{-11}$ N s/m) from the recent PEO data reported in the literature [Haley and Lodge (2005)]. This gives confidence for the self-consistency of our approach. To demonstrate the universality (even in the limit of few entanglements) and the wide range of applicability of the Milner-McLeish model, we added in Fig. 3 literature data from 32 arm PBs with higher n_e.

Concerning the recoverable compliance, data for only two PEO stars with highest n_e (32F12 and 8F11) are presented, due to torque limitations and phase angle artifacts. The data have been normalized with the plateau modulus, and are reported in Fig. 4, along with the literature data on other PB stars, as well as data for the linear chains. For the linear PEO chains with modest to high n_e, J_e^0 is found to be nearly independent from n_e, as already reported in the literature [Ferry (1980); Graessley (1993); Doi and Edwards (1986)]. On the other hand, the limited star data conform to the increasing trend of J_e^0 with arm molecular weight, due to the broadening of the modes distribution [Watanabe (1999)]. In Fig. 4 a comparison is also attempted with some normalized data on PB stars

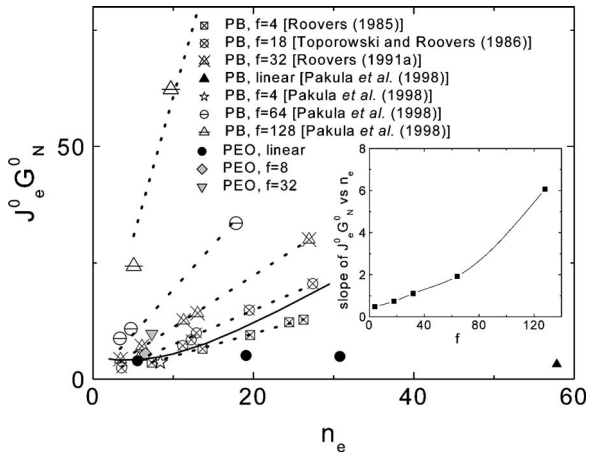

FIG. 4. Normalized recoverable compliance (with the plateau modulus) for linear and star PEOs as function of the number of entanglements per arm (a linear polymer is considered as having two arms). For comparison, data on PBd stars [Roovers (1985, 1991a); Toporowski and Roovers (1986); Pakula *et al.* (1998)] are also presented. The solid line is the MM theory. The dotted lines are drawn to guide the eye. Inset: The extracted slope of $J_e^0 G_N^0$ plotted against the star functionality.

[Roovers (1991a)] and with the predictions of the Milner-McLeish theory. Naturally, the latter does not account for any dependence of the viscoelastic properties on the number of arms. We also remark that in the range $4 < f < 32$ there is a weak effect of functionality; however, beyond $f = 32$ the effect is clearly stronger, as also suggested by the inset of Fig. 4, which depicts the slope of the J_e^0 vs. n_e data as function of the star functionality.

B. Crystallization

Following the experimental protocol explained in the Experimental section (Methods), for each crystallization temperature T_c the temperature corresponding to the endothermic peak (known as the apparent melting temperature T_m') was reported. According to Hoffman and Weeks (1962), the intercept of the regression line of the experimental data with the line $T_m' = T_c$ gives the equilibrium melting temperature T_m^0 of the polymer. The determination of T_m^0 by means of the Hoffman-Weeks method is subject to the validity of the following assumptions for the thickness ℓ of the lamellae:

$$\ell = \beta \cdot \ell^* \propto \frac{1}{T_m^0 - T_c}. \tag{1}$$

$$\ell = \text{constant on heating}, \tag{2}$$

where β is a constant, ℓ^* the thickness of the critical nucleus [Hoffman *et al.* (1959); Hoffman and Weeks (1962)], and T_c the crystallization temperature. As reported by Yamada *et al.* (2003a, 2003b), these assumptions are not always valid and in such a case the Hoffman-Weeks method does not give correct results. Although subject to the above-mentioned limitations, this procedure was followed in this work in order to get a rough estimate of the equilibrium melting temperature of the stars with respect to the linear PEO's. The results for the ideal melting temperatures are reported in Table II, whereas Fig. 5 depicts the Hoffman–Weeks procedure. Given the uncertainties and limitations discussed, these results conform well to the ideal melting temperature determined in the

TABLE II. Ideal melting points determined from the Hoffman–Weeks plot (Fig. 5) and Avrami parameters for star PEO (321 K) and linear PEO (326 K).

Sample	$\mathrm{Log}_{10} Z$	n	T_m^0 [K]
32F6	−4.80	1.9	343.5
32F12	−4.06	1.9	343.6
16F9	−4.15	1.9	342.4
8F11	−4.08	2	345.6
4F5	−5.77	2	338.6
L23	−5.27	2	346.0
L62	−4.03	2	351.4
L100	−4.96	2	345.7

literature for linear PEO [Floudas and Tsitsilianis (1997)]. A direct comparison of the various sets of experimental data in Fig. 5 suggests a lower apparent melting temperature at all crystallization temperatures for the stars as compared with the linear ones and a slight increase of the T_m' with increasing arm molecular weight as in the linear samples. The latter can be understood in terms of a thickening of the crystalline lamellae when the arm molecular weight is increased.

The evolution of the relative degree of crystallinity was extracted by means of DSC experiments, integrating the exothermic peak, after normalization with the respective limiting value at long times as

$$1 - X(t) = \frac{\Delta H_\infty - \Delta H_t}{\Delta H_\infty - \Delta H_0}, \tag{3}$$

where ΔH_∞ and ΔH_t are the latent heat on complete crystallization and after time t, respectively.

In Fig. 6 the exothermic peaks of the different samples at 321 K are shown as an example. In the inset the time evolution of the relative degree of crystallinity, $X(t)$, for all

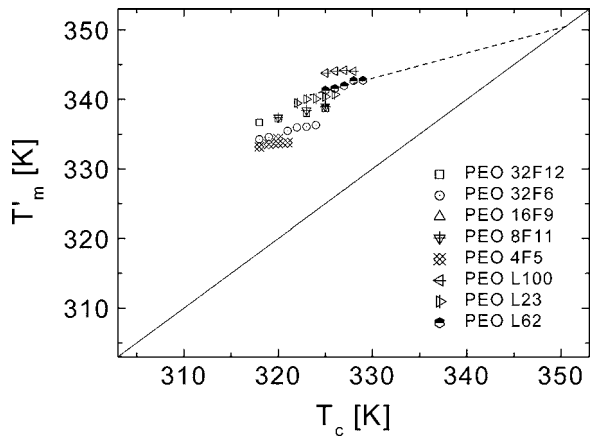

FIG. 5. Hoffman–Weeks plot for linear and star PEOs from isothermal DSC experiments. The solid line has a slope of 1; the dashed line shows the approximate T_m^0 for sample 32F12.

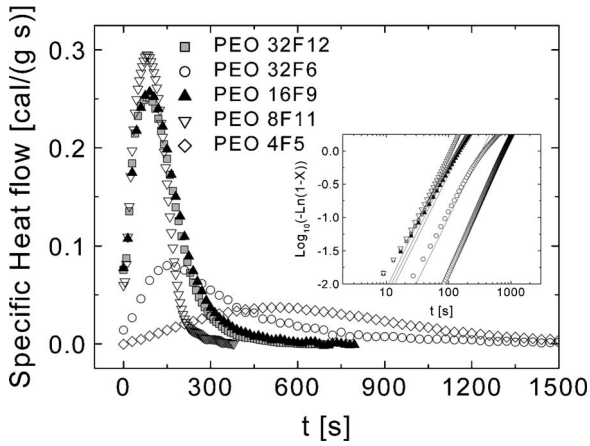

FIG. 6. Isothermal DSC curves of star PEO samples at 321 K (symbols in the figure). Inset: Avrami plot: Respective evolution of the relative degree of crystallinity (same symbols as in main figure). Solid lines are the fits to the data.

the samples is also plotted. The evolution of $X(t)$ is analyzed in the usual way, i.e., using the Kolmogorov-Avrami-Evans (KAE) equation [Kolmogoroff (1937); Avrami (1939, 1940, 1941); Evans (1945)]:

$$X = 1 - \exp(-E(t)), \tag{4}$$

where $E(t)$ denotes the volume of the "phantom crystals" grown up to time t [Avrami (1940)]. Assuming that a single mechanism of crystallization is taking place under isothermal steady state conditions, a simple expression for $E(t)$ is often used

$$E(t) = Z \cdot t^m, \tag{5}$$

where Z includes the kinetic parameters of nucleation and growth and the Avrami exponent m is the sum of the order of the time-dependent nucleation process (0 for athermal and 1 for thermal) and of the number of dimensions in which the growth is taking place. In order to extract the parameters of the KAE equation [Eq. (4)], a fitting of the experimental data in the so-called Avrami's plot (inset of Fig. 6) is needed. The Avrami approach is not valid for high values of crystalline degree $X(t)$ where impingement and secondary crystallization play a significant role. The parameters of the PEO stars are reported in Table II for the case shown in Fig. 6. The PEO stars as the linear PEO's have an Avrami's exponent close to 2, which implies disk-like growth from athermal nuclei (i.e., the initially formed crystals have a disk-like shape). The latter conclusion is based on separate kinetic experiments with polarizing optical microscopy. Therefore chain topology does not alter significantly the Avrami exponent but, as we will see below, it does affect the rate constant Z. Note that the initial disk-like crystals are finally incorporated into spherulitic macroscopic objects.

In parallel, the evolution of the relative degree of crystallinity for the linear PEO chains was also studied. Again, the Avrami plot was used to extract, by means of regressions, the parameters for the Avrami equation, and the results are reported in Table II. The three linear samples have similar Avrami exponents, close to 2. This is similar to the stars case, suggesting that the growth of crystallinity is qualitatively similar for the stars and the linear chains.

From the evolution of the relative degree of crystallinity $X(t)$, the crystallization rate can be evaluated by determining the time $t_{1/2}$ required for the crystallinity, as obtained from DSC, to reach half of its final value. This parameter can be easily expressed in terms of the two Avrami parameters Z and m

$$t_{1/2} = \left(\frac{\ln 2}{Z} \right)^{1/m}. \tag{6}$$

The half crystallization time can be determined from rheology as well. However, a direct comparison of the crystallization kinetics from rheology and DSC requires extracting the volume fraction of the time-dependent crystalline fraction $\varphi_c(t)$. In this respect we describe the rheological response by assuming a two phase system comprising an amorphous matrix and a spherulitic structure whose relative contribution evolve with time. Different models have been proposed to account for the rheological response of such composites but the simplest and limiting cases are the "series" and "parallel" models [Floudas and Tsitsilianis (1997); Alig *et al.* (1998)]. In the series (parallel) model the compliance (modulus) of the two phase system is expressed as a linear combination of the compliances (moduli) of the constituent phases as

$$J^* = (1 - \varphi_S)J_a^* + \varphi_S J_S^*,$$

$$G^* = (1 - \varphi_S)G_a^* + \varphi_S G_S^*, \tag{7}$$

where $\varphi_S(t)$ is the volume fraction of spherulites and J_a^* (G_a^*) and J_S^* (G_S^*) are the compliances (moduli) of the amorphous ($t=0$) and spherulitic ($t=\infty$) phases, respectively. Then by further assuming a constant ratio of amorphous to crystalline component in the spherulite interior, the time dependence of $\varphi_s(t)$ can be obtained from

$$\varphi_S(t) = 1 - e^{-Zt^m}. \tag{8}$$

Note that Eq. (8) is analogous to Eq. (3).

The results for the half crystallization times $t_{1/2}$, determined by DSC and rheology, are reported in Fig. 7(a). Regarding the rheological data, the half crystallization times $t_{1/2}$ were determined by applying the series and parallel models to complex compliance J^* and modulus G^* evolution during the crystallization process. In all cases, the results of the two models were quite close. Figure 7(a) depicts the data from the parallel model (which gives the longest rheological values for $t_{1/2}$), plotted against the supercooling, $T_m^0 - T$. The rheological measurements indicate a stronger temperature dependence of the $t_{1/2}$. On the other hand, this could be related also to the different range of temperatures explored. In the temperature range where it was possible to carry out both kinds of measurements at the same temperature, the data for the $t_{1/2}$ were always of the same order of magnitude. We note for completeness, that the differences between the two models in extracting $t_{1/2}$ are small but non-negligible (at most a factor of 2), but they do not influence the results and the comparison of the different polymers [Floudas *et al.* (1994); Floudas *et al.* (1996)]. Furthermore, there seems to be no change of G at long times, even after prolonged annealing [Floudas (1997)]. This suggests that, despite G being very sensitive to spherulitic growth, is not sensitive to the secondary crystallization. This is partially seen in Fig. 1, where the long-time G' value does not change with annealing time.

In Fig. 7(b) we plot the results from the linear growth rates obtained from POM for three of the stars in comparison to a linear PEO $L20$; actually, what is plotted is the product of the growth rate and the extrapolated zero-shear viscosity against the temper-

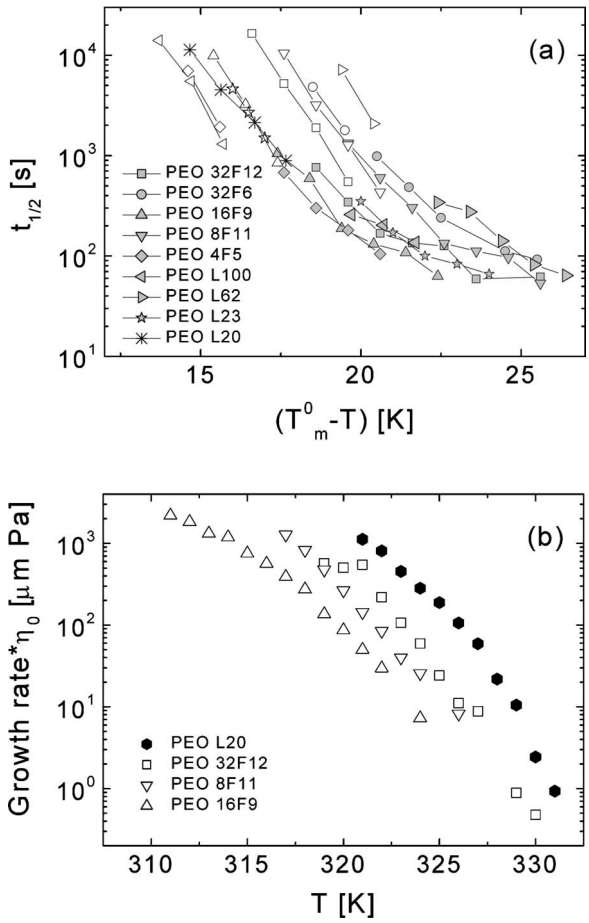

FIG. 7. (a) Half crystallization times for linear and star PEO samples. Empty symbols: DSC. Filled symbols: Rheology (the latter data are results of the parallel model). (b) Linear growth rates times zero-shear viscosities as functions of temperature (growth rates obtained from POM).

atue. Both DSC and POM results display a strong dependence of the kinetics on the chain topology (i.e., crystallization in stars is always slower than for linear chains if compared at the same temperature) and only a weak dependence on functionality. Furthermore, the temperature does not influence the crystallization kinetics (the growth rate), i.e., at all temperatures investigated the star kinetics are equally slower than for the linear chains. A last remark concerns the plot of Fig. 7(b), where the difference among the normalized growth rates may reflect the different energetic barriers for crystallization, but we note the absence of a systematic change. Same conclusions are drawn if these rates are plotted against the supercooling $T_m^0 - T$ (not shown here).

The differences observed among the $t_{1/2}$ curves of the stars in Fig. 7 can be related primarily to the arm molecular weights, whereas a much weaker effect of functionality cannot be ruled out; such an effect could be possibly imputed to secondary crystallization processes, in analogy with earlier observations on long-chain branched polyethylene [Bustos *et al.* (2006)]. However, the data are not sufficient (not high enough functionalities) to establish such an effect, and the rheology data appear more sensitive to this than the DSC and POM data. Indeed, a significant dependence of the crystallization kinetics

on the molecular weight has already been reported in the literature in the case of the linear polymers. Actually, for linear polyethylene in the molecular mass range $2.65 \times 10^4 - 2.04 \times 10^5$ g/mol, the growth rate becomes lower with increasing M_w [Hoffman (1982)]. However, in a very systematic experimental study on polyethylene fractions spanning on a wide range of M_w ($2.9 \times 10^3 - 8 \times 10^6$ g/mol), a nonmonotonic dependence of the crystallization rate on the molecular weight was observed [Ergoz *et al.* (1972)]. In particular, these authors found that increasing M_w the crystallization rate first increases rapidly then passes through a maximum and eventually decreases until reaching a plateau. This behavior was especially evident at low undercoolings.

The experimental data relative to the two stars with 32 arms (32F6 and 32F12) indicate that, in the range of arm molecular weight explored, the crystallization rate is enhanced when M_{arm} is increased. In addition, a weak effect of functionality on the crystallization kinetics can be observed. Considering, for example, the samples 8F11 and 32F12 we observe that their melting temperatures are very similar (Fig. 5) and their crystallization rates are instead different (Fig. 7). Note that in previous works, branching was recognized to have a retarding effect on crystallization and in many cases to decrease the amount of crystallinity [Cheng and Su (1993); Lambert and Phillips (1994, 1996); Chae *et al.* (2001); Bustos *et al.* (2006)].

In closing, we present a tentative interpretation of possible effects of functionality on the crystallization of star polymers. As mentioned in the Introduction, Hoffman and Miller (1988) applied the reptation concept to the estimation of the growth rate during polymer crystallization and proposed that already for the linear chains the attachment of a stem on the growing crystallite is strongly frustrated by the need for retracting the chain from the bulk. It can be expected that the same phenomenon is even more pronounced when the chain is connected to a branch point and the lamellar size is of the same order of magnitude of the whole arm. The diffusion of an arm towards the melt-crystallite interface implies the whole star motion, which is considerably affected by the functionality. Strong dependence of star diffusivity on functionality has indeed been reported in the literature for homogeneous, amorphous systems [Chen *et al.* (1999); Vlassopoulos *et al.* (2001)]. Chen *et al.* (1999) measured diffusivities of PEO stars having the same arm molecular weight but different functionality as a function of temperature. These authors found that the diffusivities followed the same temperature dependence, which could be described in terms of an Arrhenius equation

$$D = D_0 \exp\left(-\frac{E_a}{k_B T}\right), \tag{9}$$

where D_0 is a temperature-independent (reference) diffusion constant and E_a ($\sim$30 kJ/mol) is the activation energy for diffusion. The latter was identical for the PEO stars and the linear chains, however D_0 was found to be a strong function of functionality (decreasing with increasing functionality). This finding, along with the weak dependence of $t_{1/2}$ on star functionality suggests that the main effect of chain topology is to alter D_0. Chain topology, on the other hand, has minor effects on the temperature dependence on the half-crystallization time and crystal growth rates. Indeed, all star and linear PEO samples studied here, despite exhibiting strong differences in the crystallization kinetics, do show similar dependencies on temperature (Fig. 7).

IV. CONCLUDING REMARKS

The linear viscoelastic behavior of homogeneous monodisperse PEO star melts with different functionalities and arm molecular weights was studied. Compiling the present as

well as earlier data from the literature, we found a non-negligible dependence of the recoverable compliance and of the zero-shear viscosity on functionality, which was attributed to the effect of the central core. The dependence of zero-shear viscosity on the number of entanglements per arm for these systems with intermediate number and molecular weight of arms, was well described by the Milner-McLeish model, with the three molecular parameters independently justified. On the other hand, the model was less successful with the recoverable compliance, although is was qualitatively correct. It was established that for $f > 16$, the functionality does affect the linear viscoelastic properties of the star polymers.

The crystallization kinetics was investigated by means of DSC, POM and rheology experiments. A significant dependence on arm molecular weight and only a very weak dependence on functionality were observed. This was discussed in terms of simple arguments relating the half crystallization time to the overall star diffusivity, the latter depending on the functionality. The limited evidence presented here, especially concerning the arm functionality, should trigger further experimental studies on this topic, provided that appropriate model samples are available. A remaining challenge relates to whether the crystallization takes place by disentanglement process of the arms followed by chain folding and aggregation of the arms from the same star or between the different stars. This has been partly addressed in the literature with respect to star systems comprising of two crystallizable blocks (PEO and PCL) [Floudas *et al.* (1998)]. Crystallization involved first the separation of stars where only one block could crystallize and the subsequent crystal growth involving different stars. Similarly, our present experimental findings with these unique, well-defined systems, are suggestive of the star/star cooperative process. It is clear however, that further work is needed in the direction before the matter is settled.

ACKNOWLEDGMENTS

We are grateful to Jacques Roovers for providing the samples used in this work and for helpful discussions, as well as to Michael Kapnistos for valuable technical assistance. This work was carried out during two visits of S.C. to FORTH. Financial support provided by FORTH, the University of Naples "Federico II" (Programma di scambi internazionali per la Mobilità di breve durata di Docenti, Studiosi e Ricercatori; D.R. 1112-30.03.2000), the EU (HUSC network HPRN-CT2000-00017) and the Greek Ministry of Education (PYTHAGORAS I operational program) is gratefully acknowledged.

References

Acierno, S., and N. Grizzuti, "Measurements of the rheological behavior of a crystallizing polymer by an "inverse quenching" technique," J. Rheol. **47**, 563–576 (2003).

Alig, I., C. Tadjbakhsch, G. Floudas, and C. Tsitsilianis, "Viscoelastic contrast and kinetic frustration during poly(ethylene oxide) crystallization in a homopolymer and a triblock copolymer. Comparison of ultrasonic and low-frequency rheology," Macromolecules **31**, 6917–6925 (1998).

Avrami, M., "Kinetics of phase change. I. General theory," J. Chem. Phys. **7**, 1103–1112 (1939).

Avrami, M., "Kinetics of phase change. II. Transformation-time relations for random distribution of nuclei," J. Chem. Phys. **8**, 212–224 (1940).

Avrami, M., "Granulation, phase change and microstructure. Kinetics of phase change. III," J. Chem. Phys. **9**, 177–184 (1941).

Bustos, F., P. Cassagnau, and R. Fulchiron, "Effect of molecular architecture on quiescent and shear-induced crystallization of polyethylene," J. Polym. Sci., Part B: Polym. Phys. **44**, 1597–1607 (2006).

Chae, H. G., B. C. Kim, S. S. Im, and Y. K. Han, "Effect of molecular weight and branch structure on the crystallization and rheological properties of poly(butylene adipate)," Polym. Eng. Sci. **41**, 1133–1139 (2001).

Chen, E. Q., S. W. Lee, A. Q. Zhang, B. S. Moon, I. Mann, F. W. Harris, S. Z. D. Cheng, B. S. Hsiao, F. J. Yeh, E. von Merrewell, and D. T. Grubb, "Isothermal thickening and thinning processes in low-molecular-weight poly(ethylene oxide) fractions crystallized from the melt. 8. Molecular shape dependence," Macromolecules **32**, 4784–4793 (1999).

Cheng, T. L., and A. C. Su, "Spherulites of long-chain branched cis-1,4-polybutadiene," Macromolecules **26**, 7161–7166 (1993).

Clarke, N., F. R. Colley, S. A. Collins, L. R. Hutchings, and R. L. Thompson, "Self-diffusion and viscoelastic measurements of polystyrene star polymers," Macromolecules **39**, 1290–1296 (2006).

Comanita, B., B. Noren, and J. Roovers, "Star poly(ethylene oxide)s from carbosilane dendrimers," Macromolecules **32**, 1069–1072 (1999).

Coppola, S., L. Balzano, E. Gioffredi, P. L. Maffettone, and N. Grizzuti, "Effects of the degree of undercooling on flow induced crystallization in polymer melts," Polymer **45**, 3249–3256 (2004).

Doi, M., and S. F. Edwards, *The Theory of Polymer Dynamics* (Clarendon Press, Oxford, 1986).

Ergoz, E., J. G. Fatou, and L. Mandelkern, "Molecular-weight dependence of crystallization kinetics of linear polyethylene. 1. Experimental results," Macromolecules **5**, 147–157 (1972).

Evans, U. R., "The laws of expanding circles and spheres in relation to the lateral growth of surface films and the grain-size of metals," Trans. Faraday Soc. **41**, 365–374 (1945).

Ferry, J. D., *Viscoelastic Properties of Polymers* (Wiley, New York, 1980).

Fetters, L. J., A. D. Kiss, D. S. Pearson, G. F. Quack, and F. J. Vitus, "Rheological behavior of star-shaped polymers," Macromolecules **26**, 647–654 (1993).

Fetters, L. J., D. J. Lohse, D. Richter, T. A. Witten, and A. Zirkel, "Connection between polymer molecular-weight, density, chain dimensions, and melt viscoelastic properties," Macromolecules **27**, 4639–4647 (1994).

Floudas, G., T. Pakula, E. W. Fischer, N. Hadjichristidis, and S. Pispas, "Ordering kinetics in a symmetric diblock copolymer," Acta Polym. **45**, 176–181 (1994).

Floudas, G., S. Pispas, N. Hadjichristidis, T. Pakula, and I. Erukhimovich, "Microphase separation in star block copolymers of styrene and isoprene. Theory, experiment and simulation," Macromolecules **29**, 4142–4149 (1996).

Floudas, G., and C. Tsitsilianis, "Crystallization kinetics of poly(ethylene oxide) in poly(ethylene oxide) polystyrene poly(ethylene oxide) triblock copolymers," Macromolecules **30**, 4381–4390 (1997).

Floudas, G., G. Reiter, O. Lambert, and P. Dumas, "Structure and dynamics of structure formation in model triarm star block copolymers of polystyrene, poly(ethylene oxide), and poly(epsilon-caprolactone)," Macromolecules **31**, 7279–7290 (1998).

Floudas, G., L. Hilliou, D. Lellinger, and I. Alig, "Shear-induced crystallization of poly(epsilon-caprolactone). 2. Evolution of birefringence and dichroism," Macromolecules **33**, 6466–6472 (2000).

Fréchet, J. M. J., and C. J. Hawker, "Synthesis and properties of dendrimers and hyperbranched polymers," in *Comprehensive Polymer Science*, edited by G. Allen, S. L. Aggarwal, and S. Russo (Pergamon, Oxford, 1996), Vol. 2.

Graessley, W. W., and J. Roovers, "Melt rheology of 4-arm and 6-arm star polystyrenes," Macromolecules **12**, 959–965 (1979).

Graessley, W. W., "Viscoelasticity and flow in polymer melts and concentrated solutions," in *Physical Properties of Polymers*, edited by J. E. Mark (American Chemical Society, Washington, DC, 1993).

Hadinata, C., C. Gabriel, M. Ruellman, and H. M. Laun, "Comparison of shear-induced crystallization behavior of PB-1 samples with different molecular weight distribution," J. Rheol. **49**, 327–349 (2005).

Haley, J. C., and T. P. Lodge, "Dynamics of a poly(ethylene oxide) tracer in a poly(methyl methacrylate) matrix: Remarkable decoupling of local and global motions," J. Chem. Phys. **122**, 234–914 (2005).

Heck, B., T. Hugel, M. Iijima, and G. Strobl, "Steps in the formation of the partially crystalline state," Polymer **41**, 8839–8848 (2000).

Hoffman, J. D., J. J. Weeks, and W. M. Murphey, "Experimental and theoretical study of kinetics of bulk

crystallization in poly(chlorotrifluoroethylene)," J. Res. Natl. Bur. Stand., Sect. A **63A**, 67–98 (1959).

Hoffman, J. D., and J. J. Weeks, "Melting process and equilibrium melting temperature of poly(chlorotrifluoroethylene)," J. Res. Natl. Bur. Stand., Sect. A **66A**, 13 (1962).

Hoffman, J. D., "Role of reptation in the rate of crystallization of polyethylene fractions from the melt," Polymer **23**, 656–670 (1982).

Hoffman, J. D., and R. L. Miller, "Test of the reptation concept—crystal-growth rate as a function of molecular-weight in polyethylene crystallized from the melt," Macromolecules **21**, 3038–3051 (1988).

Hoffman, J. D., and R. L. Miller, "Kinetics of crystallization from the melt and chain folding in polyethylene fractions revisited: Theory and experiment," Polymer **38**, 3151–3212 (1997).

Iwata, K., "Role of entanglement in crystalline polymers 1. Basic theory," Polymer **43**, 6609–6626 (2002).

Jayakannan, M., and S. Ramakrishnan, "Effect of branching on the crystallization kinetics of poly(ethylene terephthalate)," J. Appl. Polym. Sci. **74**, 59–66 (1999).

Kapnistos, M., A. N. Semenov, D. Vlassopoulos, and J. Roovers, "Viscoelastic response of hyperstar polymers in the linear regime," J. Chem. Phys. **111**, 1753–1759 (1999).

Khanna, Y. P., "Rheological mechanism and overview of nucleated crystallization kinetics," Macromolecules **26**, 3639–3643 (1993).

Kolmogoroff, A. N., "K statisticheskoi teorii kristallizacii metallov," Izv. Akad. Nauk SSSR, Ser. Mat. **1**, 355–359 (1937).

Kornfield, J. A., G. Kumaraswamy, and A. M. Issaian, "Recent advances in understanding flow effects on polymer crystallization," Ind. Eng. Chem. Res. **41**, 6383–6392 (2002).

Kumaraswamy, G., A. M. Issaian, and J. A. Kornfield, "Shear-enhanced crystallization in isotactic polypropylene. 1. Correspondence between in situ rheo-optics and ex situ structure determination," Macromolecules **32**, 7537–7547 (1999).

Kumaraswamy, G., "Crystallization of polymers from stressed melts," J. Macromol. Sci., Polym. Rev. **C45**, 375–397 (2005).

Lambert, W. S., and P. J. Phillips, "Crystallization kinetics of low-molecular-weight fractions of branched polyethylenes," Macromolecules **27**, 3537–3542 (1994).

Lambert, W. S., and P. J. Phillips, "Crystallization kinetics of fractions of branched polyethylenes.2. Effect of molecular weight," Polymer **37**, 3585–3591 (1996).

Lellinger, D., G. Floudas, and I. Alig, "Shear induced crystallization in poly(epsilon-caprolactone): Effect of shear rate," Polymer **44**, 5759–5769 (2003).

Masuda, T., Y. Ohta, and S. Onogi, "Rheological properties of anionic polystyrenes. III. Characterization and rheological properties of four-branch polystyrenes," Macromolecules **4**, 763–768 (1971).

McLeish, T. C. B., "Tube theory of entangled polymer dynamics," Adv. Phys. **51**, 1379–1527 (2002).

McLeish, T. C. B., "Why and when does dynamic tube dilation work for stars?," J. Rheol. **47**, 177–198 (2003).

McLeish, T. C. B., "A theory for heterogeneous states of polymer melts produced by single chain crystal melting," Soft Matter **3**, 83–87 (2007).

Merrill, E. W., in *Poly(ethylene glycol) Chemistry: Biotechnical and Biomedical Applications*, edited by J. M. Harris (Plenum, New York, 1992).

Milner, S. T., and T. C. B. McLeish, "Parameter-free theory for stress relaxation in star polymer melts," Macromolecules **30**, 2159–2166 (1997).

Milner, S. T., and T. C. B. McLeish, "Arm-length dependence of stress relaxation in star polymer melts," Macromolecules **31**, 7479–7482 (1998).

Nuñez, E. F., E. Malmstrom, H. Claesson, P.-E. Werner, and U. W. Gedde, "Crystal structure, melting behavior and equilibrium melting point of star polyesters with crystallisable poly(ε-caprolactone) arms," Polymer **45**, 5251–5263 (2004).

Ohta, Y., T. Masuda, and S. Onogi, "Rheological properties of anionic polystyrenes. 12. Viscosity and steady-state compliance of multibranched star polystyrenes," Polym. J. (Tokyo, Jpn.) **18**, 337–346 (1986).

Pakula, T., S. Geyler, T. Edling, and D. Boese, "Relaxation and viscoelastic properties of complex polymer systems," Rheol. Acta **35**, 631–644 (1996).

Pakula, T., D. Vlassopoulos, G. Fytas, and J. Roovers, "Structure and dynamics of melts of multiarm polymer stars," Macromolecules **31**, 8931–8940 (1998).

Pogodina, N. V., and H. H. Winter, "Polypropylene crystallization as a physical gelation process," Macromolecules **31**, 8164–8172 (1998).

Pryke, A., R. J. Blackwell, T. C. B. McLeish, and R. N. Young, "Synthesis, hydrogenation, and rheology of 1,2-polybutadiene star polymers," Macromolecules **35**, 467–472 (2002).

Psarski, M., E. Piorkowska, and A. Galeski, "Crystallization of polyethylene from melt with lowered chain entanglements," Macromolecules **33**, 916–932 (2000).

Qiao, X., T. Sawada, Y. Matsumiya, and H. Watanabe, "Constraint release in moderately entangled monodisperse star polyisoprene systems," Macromolecules **39**, 7333–7341 (2006).

Raju, V. R., H. Rachapudy, and W. W. Graessley, "Properties of amorphous and crystallizable hydrocarbon polymers. 4. Melt rheology of linear and star-branched hydrogenated polybutadiene," J. Polym. Sci., Part B: Polym. Phys. **17**, 1223–1235 (1979).

Rastogi, S., D. R. Lippits, G. W. Peters, R. Graf, Y. Yao, and H. W. Spiess, "Heterogeneity in polymer melts from melting of polymer crystals," Nat. Mater. **4**, 635–641 (2003).

Righetti, M. C., and A. Munari, "Influence of branching on melting behavior and isothermal crystallization of poly(butylene terephthalate)," Macromol. Chem. Phys. **198**, 363–378 (1997).

Risch, B. G., G. L. Wilkes, and J. M. Warakomski, "Crystallization kinetics and morphological features of star-branched nylon-6—Effect of branch-point functionality," Polymer **34**, 2330–2343 (1993).

Roovers, J., "Properties of the plateau zone of star-branched polybutadienes and polystyrenes," Polymer **26**, 1091–1095 (1985).

Roovers, J., "Viscoelastic properties of 32-arm star polybutadienes," Macromolecules **24**, 5895–5896 (1991a).

Roovers, J., "Melt rheology of highly branched polymers," J. Non-Cryst. Solids **131**, 793–798 (1991b).

Santangelo, P. G., C. M. Roland, and J. E. Puskas, "Rheology of star-branched polyisobutylene," Macromolecules **32**, 1972–1977 (1999).

Seguela, R., "Critical review of the molecular topology of semicrystalline polymers: The origin and assessment of intercrystalline tie molecules and chain entanglements," J. Polym. Sci., Part B: Polym. Phys. **43**, 1729–1748 (2005).

Slot, J. J. M., and P. A. M. Steeman, "Rheology of polydisperse star polymer melts: Extension of the parameter-free tube model of Milner and McLeish to arbitrary arm-length polydispersity," Macromol. Theory Simul. **14**, 387–399 (2005).

Stiriba, S.-E., H. Frey, and R. Haag, "Dendritic polymers in biomedical applications: From potential to clinical use in diagnostics and therapy," Angew. Chem., Int. Ed. **41**, 1329–1334 (2002).

Strobl, G., "From the melt via mesomorphic and granular crystalline layers to lamellar crystallites: A major route followed in polymer crystallization?," Eur. Phys. J. E **3**, 165–183 (2000).

Tanner, R. I., "On the flow of crystallizing polymers I. Linear regime," J. Non-Cryst. Solids **112**, 251–268 (2003).

Toporowski, P. M., and J. Roovers, "Synthesis and properties of eighteen-arm polybutadienes," J. Polym. Sci., Part A: Polym. Chem. **24**, 3009–3019 (1986).

van Meerveld, J., G. W. M. Peters, and M. Hutter, "Towards a rheological classification of flow induced crystallization experiments of polymer melts," Rheol. Acta **44**, 119–134 (2004).

Vega, D. A., J. M. Sebastian, W. B. Russel, and R. A. Register, "Viscoelastic properties of entangled star polymer melts: Comparison of theory and experiment," Macromolecules **35**, 169–177 (2002).

Vlassopoulos, D., G. Fytas, T. Pakula, and J. Roovers, "Multiarm star polymers dynamics," J. Phys.: Condens. Matter **13**, R855–R876 (2001).

Watanabe, H., "Viscoelasticity and dynamics of entangled polymers," Prog. Polym. Sci. **24**, 1253–1403 (1999).

Watanabe, H., T. Sawada, and Y. Matsumiya, "Constraint release in star/star blends and partial tube dilation in monodisperse star systems," Macromolecules **39**, 2553–2561 (2006).

Yamada, K., M. Hikosaka, A. Toda, S. Yamazaki, and K. Tagashira, "Equilibrium melting temperature of isotactic polypropylene with high tacticity: 1. Determination by differential scanning calorimetry," Macromolecules **36**, 4790–4801 (2003a).

Yamada, K., M. Hikosaka, A. Toda, S. Yamazaki, and K. Tagashira, "Equilibrium melting temperature of isotactic polypropylene with high tacticity. 2. Determination by optical microscopy," Macromolecules **36**, 4802–4812 (2003b).

Yamazaki, S., M. Hikosaka, A. Toda, I. Wataoka, and F. Gu, "Role of entanglement in nucleation and 'melt relaxation' of polyethylene," Polymer **43**, 6585–6593 (2002).

Yamazaki, S., F. M. Gu, K. Watanabe, K. Okada, A. Toda, and M. Hikosaka, "Two-step formation of entanglement from disentangled polymer melt detected by using nucleation rate," Polymer **47**, 6422–6428 (2006).

Zhao, S., X. Zhang, and G. Jin, "Influence of molecular structure of star S-SBR on its properties," J. Appl. Polym. Sci. **89**, 2311–2315 (2003).